*Fifth International Conference on CFD in the Process Industries*
*CSIRO, Melbourne, Australia*
*13-15 December 2006*

# HEMODYNAMICS AND STRESS DISTRIBUTION IN A CEREBRAL ANEURYSM PARTIALLY BLOCKED WITH COILS

**Shakil AHMED[1], Ilija D. ŠUTALO[1] and Helen KAVNOUDIAS[2]**

[1]Commonwealth Scientific and Industrial Research Organisation (CSIRO), Highett, VIC 3190, AUSTRALIA
[2]Radiology Department, The Alfred, Commercial road, Melbourne, VIC 3004, AUSTRALIA

## ABSTRACT

Stroke due to subarachnoid haemorrhage from ruptured cerebral aneurysms is one of the highest causes of death and economic burden in our society. Aneurysms can be treated by placing coils in the aneurysm to alter the local hemodynamics and lower the wall shear stresses to make the aneurysmal flow inactive. Although velocity measurements have been previously made in models of cerebral aneurysms, no specific information is available for the stress distribution inside lateral aneurysms. A three-dimensional Computational Fluid Dynamics (CFD) model was used to investigate the hemodynamics of a pear shaped lateral cerebral aneurysm partially blocked with coils. Stress distribution for different coil locations inside the aneurysm was investigated by using uni-directional Fluid Structure Interaction (FSI). The wall pressure obtained from the CFD was used as a boundary condition for structural analysis. The results were analysed in terms of inflow rate, wall shear stress, apparent viscosity and effective (Von-Mises) stress. The predictions showed areas of the aneurysm that experience high stress. CFD has been shown to be a valuable tool that could help predict which aneurysms would require additional treatment.

## NOMENCLATURE

| | |
|---|---|
| $q$ | constant |
| $r$ | radius of the parent vessel |
| $\alpha$ | Womersley number |
| $\gamma$ | shear rate |
| $\lambda$ | constant |
| $\mu$ | coefficient of viscosity |
| $\mu_\alpha$ | constant |
| $\mu_o$ | constant |
| $\nu$ | kinematic viscosity |
| $\sigma_{von}$ | Von-Mises stress |
| $\sigma_1, \sigma_2, \sigma_3$ | principal stresses |
| $\omega$ | angular velocity |

## INTRODUCTION

There is no specific methodology that can assist neurosurgeon or neuroradiologist in decision-making for the treatment of cerebral aneurysms. Decision to treat is arbitrary and dependent on their experience. Currently 50% of cerebral aneurysms are treated with open surgery utilising small metal clips which seal the aneurysmal sac (clipping) and 50% are treated with the less invasive interventional technique of inserting coils into the aneurysmal sac. The placement of the coils in the arteries harboring aneurysms and across the orifices of aneurysms is intended for effectively altering the local hemodynamics, such as making the intra aneurysmal flow inactive, lowering the wall shear stresses, promoting the formation of thrombus inside the aneurysm, and, in turn, excluding the aneurysm from cardiac circulation.

In recent years various attempts have been made (Byun and Rhee, 2003, 2004; Gobin et al., 1994) to locate the optimum position of the coils, especially for giant aneurysms where it is difficult to fill an aneurysm sac completely with coils. Investigations on cerebral aneurysms (Liou and Liao, 1997; Hoi et al., 2004) revealed that lateral aneurysms arising from a large curvature parent vessel are more risky than those of arising from a straight or small-curvature parent vessel. Some theoretical models (Gao et al., 1997) of the cerebral circulation, based on both hydrodynamics and electrical network analysis, have been developed to investigate the influences on regional cerebral hemodynamics. Although extensive experimental and numerical investigations (Liou et al., 1997; Liou and Liou, 2004; Lieber and Gounis, 2002; Tateshima et al., 2001, 2003, 2004; Cebral et al., 2003; Castro et al., 2006; Moore et al., 2006) of flow velocity and flow visualization have been made on lateral cerebral aneurysms no specific information is available for stress distribution inside aneurysms. There are substantially fewer papers (De Martino et al., 2001; Li and Kleinstreuer, 2005; Valencia and Solis, 2006; Torii et al., 2006) dealing with FSI between the blood and the aneurysm wall. Martino et al. (2001) and Li and Kleinstreuer (2005) investigated the FSI on abdominal aortic aneurysms. Valencia and Solis (2006) described the flow dynamics and arterial wall interaction of a terminal aneurysm of the basilar artery and compared its wall shear stress, pressure, effective stress and wall deformation with those of a healthy basilar artery. Torii et al. (2006) studied the FSI of a cerebral aneurysm located in the left middle cerebral arterial bifurcation for high blood pressure and found that hypertension affects the growth of an aneurysm and the damage in arterial tissues. But the flow was modelled as Newtonian. No information is available in the literature for FSI on lateral cerebral aneurysm. The hemodynamics inside aneurysms is very complex and needs detailed investigation.

## LATERAL CEREBRAL ANEURYSM GEOMETRY

Cerebral aneurysms are frequently observed in the outer wall of curved vessels, e.g. the internal carotid artery (ICA), and near the apex of bifurcated vessels, e.g. the

anterior communicating artery and the middle cerebral artery. This paper presents the CFD investigation of a pear shaped ICA lateral cerebral aneurysm. An average size cerebral aneurysm with straight parent vessel was chosen for this investigation. The neck width, dome diameter, height and artery diameter were 3.2 mm, 5.4 mm, 5.4 mm and 3.2 mm respectively. Coils are usually made of platinum or Ni-Ti wire that has self-expanding properties and shape-memory capabilities. It can be compressed into a line and introduced into the micro-catheter. After progressing into the aneurysm neck, it will emerge from the tip of the micro-catheter and recover its previously defined shape and size. In this investigation it was assumed that the coils were densely packed. Based on this assumption the inserted coils were modelled as a sphere. The aneurysm was partially filled with the coils and the diameter of the sphere was three fourths of the dome diameter. The coils were placed in two positions, first at the proximal neck and then at the distal neck. Due to symmetry only half of the aneurysm model was simulated which reduced the computational cost and time. All three models are shown in figure 1.

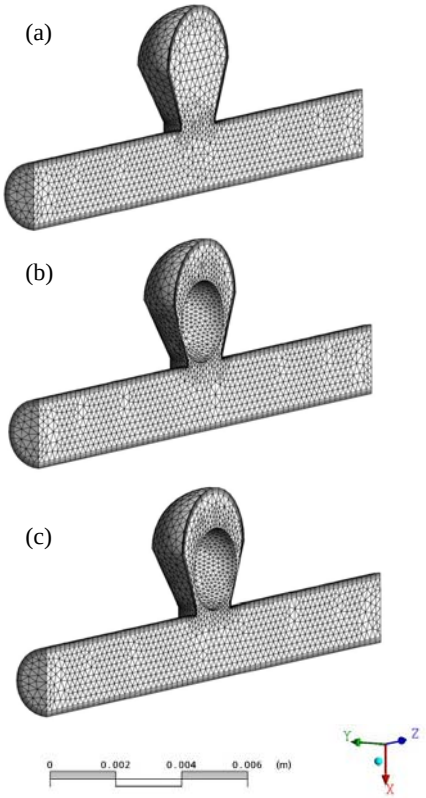


**Figure 1**: Aneurysm grid for the fluid flow analysis: (a) without coils (b) coils at proximal neck and (c) coils at distal neck. Flow left to right.

## NUMERICAL MODELLING

For the fluid domain three-dimensional transient incompressible laminar flow fields were obtained by solving the continuity and Navier-Stokes equations. Numerical modelling was performed using a commercially available CFD package ANSYS-CFX which has a coupled solver and uses an unstructured grid based on the finite volume method. The inlet boundary condition was set by specifying a velocity pulse (William, 2001) at the inlet for a period of 0.8 s. The inlet velocity was applied at five diameters upstream of the aneurysm and was nearly fully developed at two diameters upstream of the aneurysm. The maximum and mean of the Reynolds numbers based on the parent vessel diameter were 560 and 110 respectively and the Womersley number ( $\alpha = r\sqrt{\omega/\nu}$ ), which characterizes the pulsatility of the flow, was 7.5. The Reynolds number at the neck of the aneurysm at peak systole was 15. A pressure pulse (William, 2001) was applied at the outlet. All boundary conditions and the fully developed velocity profile at the peak systole upstream of two diameters are shown in figure 2.

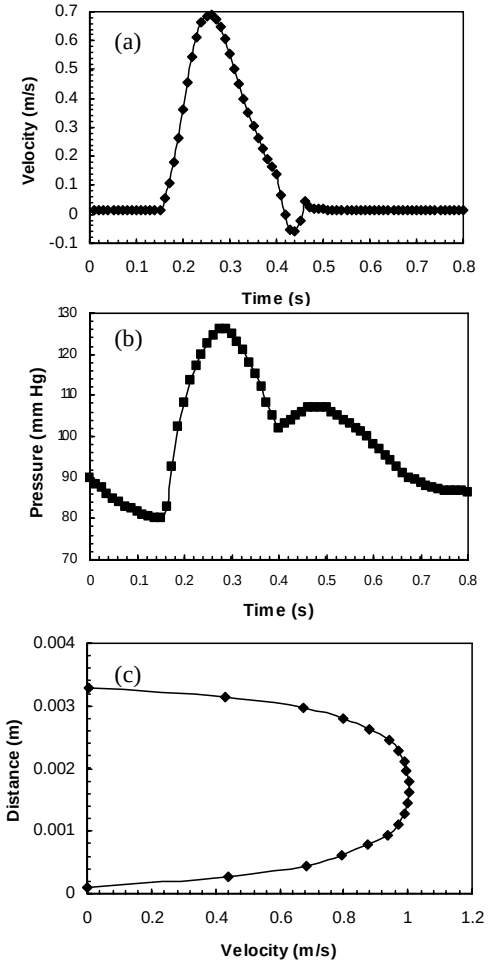


**Figure 2**: Boundary conditions for (a) inlet (b) outlet and (c) velocity profile at the peak systole (0.26 s) in the symmetry plane at two diameters upstream of the aneurysm model without coils.

The density of the blood was 1050 kg/m$^3$. Since blood consists in a suspension of particles in an aqueous medium, it behaves as a non-Newtonian fluid. The non-Newtonian behaviour of blood was modelled by using Carreau's model which is

$$\frac{\mu - \mu_\alpha}{\mu_o - \mu_\alpha} = [1.0 + (\lambda\gamma)^2]^{\frac{(q-1)}{2}} \quad (1)$$

All the parameters for Carreau model were taken from Byun and Rhee (2004). The time step used for this simulation was 0.0002 s and the convergence criteria for all variables were $10^{-3}$. Cerebral arteries are less elastic than other large arteries (Hayashi et al., 1980). Therefore the change in fluid domain due to deformation of the artery wall is negligible so it was reasonable to use uni-

directional FSI to calculate the stress inside the aneurysm wall. The wall pressure obtained from CFD was used as a boundary condition in the structural analysis.

For the structural analysis commercially available software ANSYS-MULTIPHYSICS was used. The governing equation for the structural domain was the momentum conservation equation. The artery wall was assumed to be elastic, isotropic, incompressible and homogeneous with a density of 1050 kg/m$^3$ and a Poisson's ratio of 0.45 (De Martino et al., 2001). The non-linear deformation of the artery wall was considered in this investigation. Experimental results of elasticity studies in an aneurysm show that the Young's Modulus is as high as 300 MPa compared to 1 MPa for a normal artery (Valencia and Solis, 2006). The value of the Young's Modulus was taken as 5 MPa with a wall thickness of 0.2 mm. Two ends of the artery were held fixed by specifying zero-displacement boundary conditions. These restrictions were applied far from the aneurysm and therefore did not affect the aneurysm deformation and effective stress calculation in the aneurysm wall. The symmetry boundary condition was applied at the symmetry plane. The model for the structural analysis is shown in figure 3. In order to analyse the stress distribution in the aneurysm wall, the Von-Mises stress, used as a material fracture criteria in complicated geometries, was employed.

$$\sigma_{Von} = \frac{\sqrt{2}}{2}\sqrt{(\sigma_1-\sigma_2)^2+(\sigma_2-\sigma_3)^2+(\sigma_3-\sigma_1)^2} \quad (2)$$

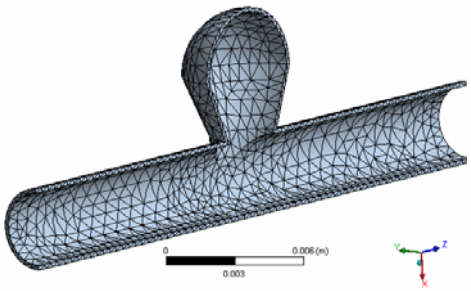

**Figure 3**: Aneurysm grid for structural analysis.

### Grid Independence Test

For the fluid model the grid consisted of tetrahedral and prismatic elements. The grid independence test was performed on aneurysm models and the solutions were grid independent when the total number of elements was 37024 for aneurysm model without coils and 40816 for aneurysm model with coils. Starting with a coarse grid the number of elements was increased gradually and each time velocity profile upstream of two diameters of aneurysm was plotted. When the velocity profile for two successive grid refinements was unchanged the solutions were grid independent. For the structural analysis the total number of elements used was 3654.

## RESULTS AND DISCUSSIONS

### Flow Dynamics

In the aneurysm model without coils, at the early acceleration phase blood was introduced into the aneurysm through the proximal neck (left side) and exited to the parent artery through the distal neck (right side). Inflow into the aneurysm then gradually moved towards the distal neck. At the mid acceleration phase most of the blood drawn from the distal neck moved out from the proximal neck, while a portion of the blood formed a recirculation inside the aneurysm sac. At the peak systole inflow from the distal neck was increased and the centre of the recirculation moved towards the distal neck. During the deceleration phase the fluid flow pattern did not change significantly.

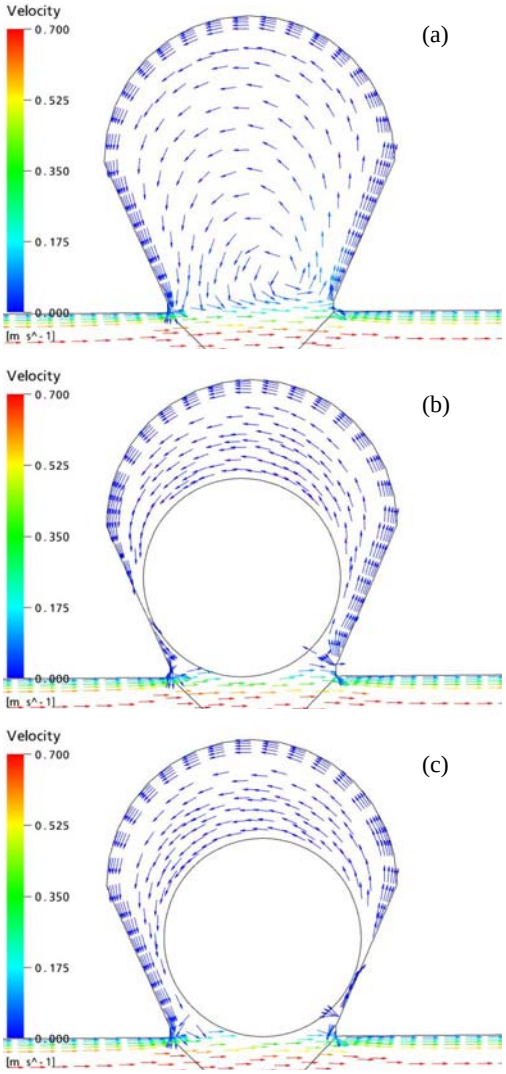


**Figure 4**: Comparison of the predicted velocity vectors at the peak systole (0.26 s) in the symmetry plane for (a) aneurysm model without coils (b) coils at proximal neck and (c) coils at distal neck.

Figure 4 shows the comparison of the predicted velocity vectors at the peak systole (0.26 s) in the symmetry plane with and without coils inside the aneurysm sac. For coils at the proximal neck the blood was introduced through the distal neck and came out through the side wall of the coils while inflow from the side wall of the coils exited to the parent vessel through the proximal neck for coils at distal neck. The noticeable change was the absence of recirculation in both coil cases. The flow from the inlet impinged the aneurysm wall at the distal neck and then divided into two parts. One part entered into the aneurysm sac while the other moved straight into the parent vessel. As a result a high velocity gradient existed in this region. The inflow into the aneurysm sac is an important criterion for the endovascular treatment of cerebral aneurysms as controlling the blood flow at the inflow region is a major

step in achieving permeant occlusion of an aneurysm. Inflow rate at the peak systole (0.26 s) from the parent vessel into the aneurysm sac was calculated by averaging the velocity components normal to the aneurysm neck plane. For aneurysm model without coils the inflow rate was 6.11 x $10^{-8}$ $m^3/s$ and was reduced by 51% (2.99 x $10^{-8}$ $m^3/s$) and 53% (2.85 x $10^{-8}$ $m^3/s$) for coils at proximal neck and distal neck respectively.

Blood is a non-Newtonian fluid whereby its viscosity varies with shear stress. This flow behaviour of blood occurs because of the existence of red blood cells. At high shear stress red blood cells are disaggregated and blood acts as a Newtonian fluid but at low shear stress red blood cells aggregate, apparent viscosity increases, and blood behaves like a non-Newtonian fluid. The flow velocity inside the aneurysm, especially in the dome, was very low and the flow was almost stagnant in this region. Apparent viscosity can play an important role in thrombus formation in this region. Figure 5 shows the comparison of apparent viscosity at the peak systole (0.26 s) in the symmetry plane between the aneurysm models with and without coils. The apparent viscosity increased significantly after the coils were placed inside the aneurysm sac. The maximum apparent viscosity was almost doubled and occurred at the proximal dome for coils at the proximal neck and the distal dome for coils at the distal neck. As the blood entered into the aneurysm sac the velocity was reduced due to coils, apparent viscosity increased, which in turn additionally reduced the velocity and we expect will promote more thrombosis to be formed.

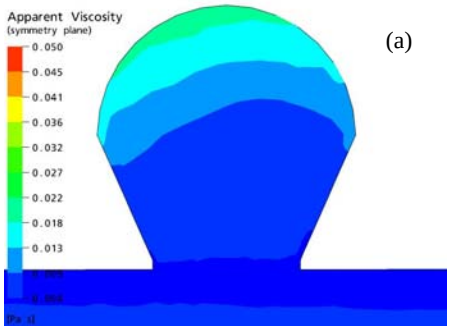


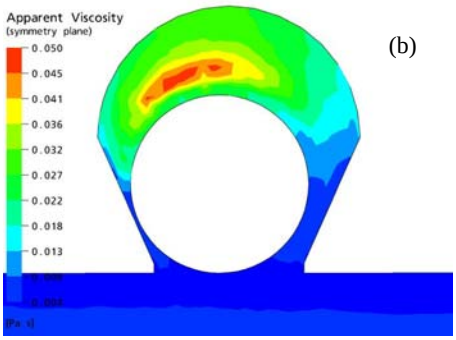


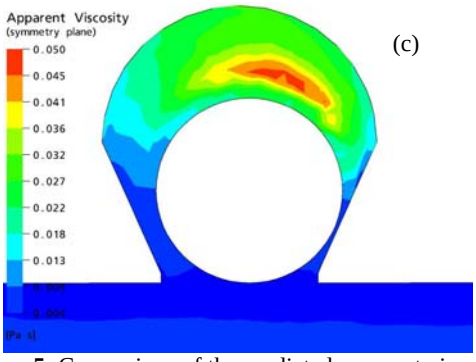


**Figure 5**: Comparison of the predicted apparent viscosity at the peak systole (0.26 s) in the symmetry plane for (a) aneurysm model without coils (b) coils at proximal neck and (c) coils at distal neck.

Hemodynamic stress is believed to be one of the important factors in the formation and growth of aneurysms. Figure 6 shows the wall pressure and wall shear stress (WSS) distribution at the peak systole (0.26 s) in the symmetry plane for coils at the distal neck. The wall pressure distribution was independent of coil location for these two cases so only the wall pressure for coils at the distal neck has been shown here. The pressure at the aneurysm wall was almost same (difference 1 mm Hg) to that in the parent artery. The WSS inside the aneurysm sac was low and was maximum (19.8 Pa) at the distal neck consistent with the results of Gobin et al. (1994) and Torii et al. (2006). At high shear stress the velocity as well as shear rate is high, the apparent viscosity is nearly constant and the blood acts as a Newtonian fluid. The high WSS in this region occurred due to the high velocity gradient which has been described earlier.

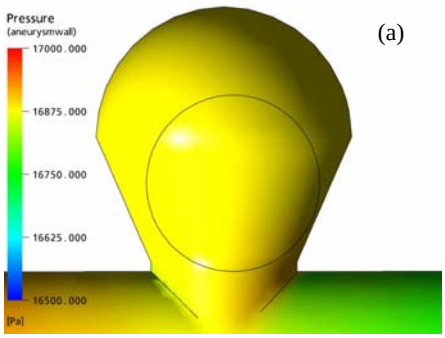


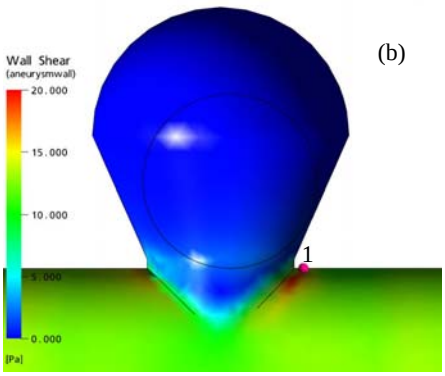


**Figure 6**: Distribution of (a) wall pressure and (b) WSS at the peak systole (0.26 s) in the symmetry plane for coils at the distal neck.

Figure 7 shows the variation of maximum WSS between the aneurysm models with and without coils for one cardiac cycle. At the peak systole (0.26 s) the maximum WSS was 21.5 Pa before the coils were placed. The maximum WSS was reduced by 2% (21.1 Pa) and 8.2% (19.8 Pa) for coils placed at the proximal and distal neck respectively. For all cases the location of the maximum WSS was near the distal neck as shown in figure 6(b), point 1.

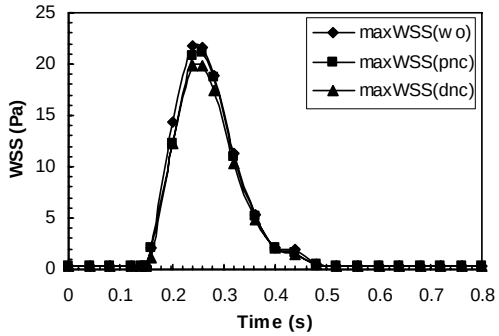


**Figure 7**: Comparison of maximum WSS between the aneurysm models without coils (wo), coils at proximal neck (pnc) and coils at distal neck (dnc) for one cardiac cycle.

## Solid Dynamics

The deformation at the peak systole (0.26 s) due to unsteady blood pressure is shown in figure 8(a). The deformation was independent of coil location for these two cases so only the deformation for coils at the distal neck is shown in figure 8(a). The deformation was larger around the aneurysm sac. The maximum deformation occurred in the parent vessel just below the aneurysm neck plane and was equal to the thickness of the artery wall.

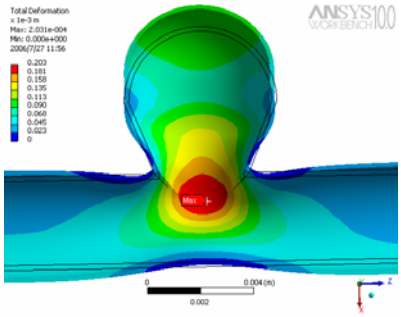

(a)

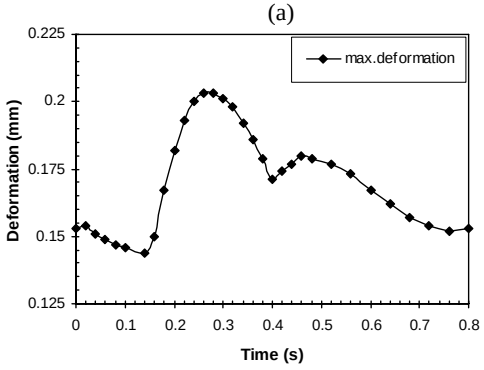


(b)

**Figure 8**: (a) Deformation at the peak systole (0.26 s) and (b) variation of maximum deformation for coils at the distal neck.

Figure 8(b) shows the variation of the maximum deformation for one cardiac cycle. The distribution of maximum deformation closely resembled the pressure profile. Figure 9(a) shows the effective (Von-Mises) stress distribution at the peak systole (0.26 s) for coils at the distal neck. Like WSS the maximum stress occurred at the distal neck and was also independent of coil location. The value of the maximum effective stress was around 0.62 MPa.

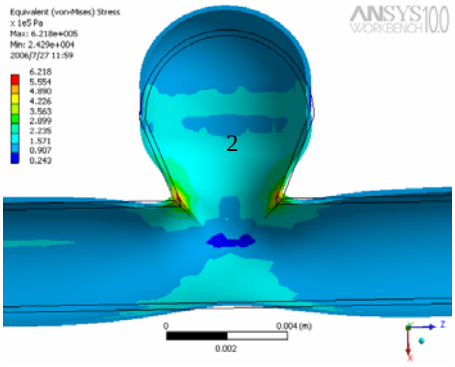


(a)

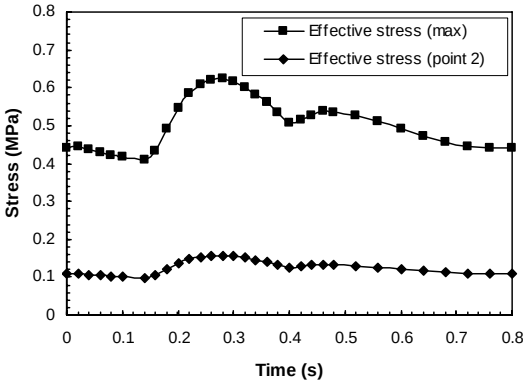


(b)

**Figure 9**: (a) Effective stress at the peak systole (0.26 s) and (b) variation of effective stress for coils at the distal neck.

Investigation of the cerebral aneurysm revealed that rupture of the aneurysm occurs in the dome rather than at the neck. For this reason variation of the maximum effective stress as well as effective stress at a point (figure 9(a), point 2) inside the dome for one cardiac cycle was calculated and compared in figure 9(b). At peak systole (0.26 s) the effective stress at point 2 was 75% lower (0.157 MPa) compared to the maximum effective stress. In both cases the stress distribution was similar to the pressure profile.

## CONCLUSION

Multiple factors must be taken into account when modelling an aneurysm: the structure of the artery wall, the pressure, hemodynamic stress, the flow dynamics and the geometry of the parent artery. In this investigation an attempt was made to determine suitable coil locations inside the giant aneurysm when the aneurysm was partially filled with coils. Stress distribution for different coil locations inside the aneurysm was investigated and the location for maximum stress was determined. It was found that the wall shear stress and the effective stress were highest at the distal neck, but in most cases rupture

occurs inside the dome. The wall pressure inside the aneurysm was similar to that of parent artery whether or not coils were present within it at the two coils position considered. An increase in the parent artery pressure (emotional strain, hypertension) will increase the wall pressure inside the aneurysm. As the effective stress distribution follows the pressure profile the effective stress will also increase inside the aneurysm. When the coils were placed inside the aneurysm the inflow was reduced at the neck plane. The reduction in flow was slightly higher for coils at the distal neck compared to that of the proximal neck. The apparent viscosity inside the aneurysm sac was increased which additionally reduced the flow and we expect the thrombus will form in the dome. The maximum wall shear stress was lower in case of distal neck coils. Controlling the blood flow at the inflow region is an important step in achieving permanent occlusion. In this investigation coils were placed in two locations and it was assumed that the parent artery was straight. For curved parent artery as well as for coils placed at the proximal and distal dome will change the hemodynamics. More investigation is required to determine the optimum coil location inside the giant cerebral aneurysm.

## REFERENCES


BYUN, H.S. and RHEE, K., (2003), "Intraaneurysmal flow changes affected by clip location and occlusion magnitude in a lateral aneurysm model", *Medical Engineering & Physics*, **25**, 581-589.

BYUN, H.S. and RHEE, K., (2004), "CFD modeling of blood flow following coil embolization of aneurysms", *Medical Engineering & Physics*, **26**, 755-761.

CASTRO, M.A., PUTMAN, C. M. and CEBRAL, J. R., (2006), "Patient-Specific Computational Modeling of Cerebral Aneurysms With Multiple Avenues of Flow From 3D Rotational Angiography Images", *Academic Radiology*, **13/7**, 811-821.

CEBRAL, J. R., CASTRO, M. A., SOTO, O., LOHNER, R. and ALPERIN, N., (2003), "Blood-flow models of the circle of Willis from magnetic resonance data", *Journal of Engineering Mathematics*, **47**, 369-386.

DE MARTIONO, E.S., GUADAGNI, G., FUMERO, A., BALLERINI, G., SPIRITO, R., BIGLIOLI, P. and REDAELLI, A., (2001), "Fluid-structure interaction within realistic three-dimensional models of the aneurysmatic aorta as a guidance to assess the risk of rupture of the aneurysm", *Medical Engineering & Physics*, **23**, 647-655.

GAO, E., YOUNG, W.L., ORNSTEIN, E., SPELLMAN, J.P. and MA, Q., (1997), "A Theoretical Model of Cerebral Hemodynamics: Application to the Study of Arteriovenous Malformations", *Journal of Cerebral Blood Flow and Metabolism*, **17**, 905-918.

GOBIN, Y.P., COUNORD, J.L., FLAUD, P. and DUFFAUX, J., (1994), "In vitro study of haemodynamics in a giant saccular aneurysm model: influence of flow dynamics in the parent vessel and effects of coil embolisation", *Neuroradiology*, **36**, 530-536.

HAYASHI, K., HANDA, H., NAGASAWA, S., OKUMURA, A. and MORITAKE, K., (1980), "Stiffness and elastic behaviour of human intracranial and extracranial arteries", *Journal of Biomechanics*, **13**, 175-184.

HOI, Y., MENG, H., WOODWARD, S.H., BENDOK, B.R., HANEL, R.A., GUTERMAN, L.R. and HOPKINS, L.N., (2004), "Effects of arterial geometry on aneurysm growth: three-dimensional computational fluid dynamics study", *J. Neurosurg*, **101**, 676-681.

LI, Z. and KLEINSTREUER, C., (2005), "Blood flow and structure interactions in a stented abdominal aortic aneurysm model", *Medical Engineering & Physics*, **27**, 369-382.

LIEBER, B.B. and GOUNIS, M.J., (2002) "The physics of endoluminal stenting in the treatment of cerebrovascular aneurysms", *Neurological Research*, **24/1**, 33-42.

LIOU, T.-M. and LIAO, C.-C., (1997), "Flowfields in lateral aneurysm models arising from parent vessels with different curvatures using PTV", *Experiments in Fluids*, **23**, 288-298.

LIOU, T.-M. and LIOU S.-N., (2004), " Pulsatile Flows in a Lateral Aneurysm Anchored on a Stented and Curved Parent Vessel", *Experimental Mechanics*, **44/3**, 253-260.

LIOU, T.-M., CHANG, W.-C. and LIAO, C.-C., (1997), "Experimental Study of Steady and Pulsatile Flows in Cerebral Aneurysm Model of Various Sizes at Branching Site", *Journal of Biomechanical Engineering*, **119**, 325-332.

MOORE, S., DAVID, T., CHASE, J.G.,ARNOLD, J. and FINK, J., (2006), "3D models of blood flow in the cerebral vasculature", *Journal of Biomechanics*, **39**, 1454-1463.

TATESHIMA, S., GRINSTEAD, J., SINHA, S., NIEN, Y.L., MURAYAMA, Y., VILLABLANCA, J.P., TANISHITA, K. and VINUELA, F., (2004), "Intraaneurysmal flow visualization by using phase-contrast magnetic resonance imaging: feasibility study based on a geometrically realistic in vitro aneurysm model", *J. Neurosurg*, **100**, 1041-1048**.**

TATESHIMA, S., MURAYAMA, Y., VILLABLANCA, J.P., MORINO, T., TAKAHASHI, H., YAMAUCHI, T., TANISHITA, K. and VINUELA, F., (2001), "Intraaneurysmal flow dynamics study featuring an acrylic aneurysm model manufactured using a computerized tomography angiogram as a mold", *J. Neurosurg*, **95**, 1020-1027.

TATESHIMA, S., VINUELA, F., VILLABLANCA, J.P., MURAYAMA, Y., MORINO, T., NOMURA, K. and TANISHITA, K., (2003), "Three-dimensional blood flow analysis in a wide-necked internal carotid artery-ophthalmic artery aneurysm", *J Neurosurg*, **99**, 526-533.

TORII, R., OSHIMA, M., KOBAYASHI, T., TAKAGI, K. and TEZDUYAR, T. E., (2006), "Fluid-structure interaction modeling of aneurysmal conditions with high and normal blood pressures", *Comput. Mech.*, **38**, 482-490.

VALENCIA, A. and SOLIS, F., (2006), "Blood flow dynamics and arterial wall interaction in a saccular aneurysm model of the basilar artery", *Computers and Structures*, **84**, 1326-1337.

WILLIAM, F.G., (2001), "Review of Medical Physiology", *21st International Edition*, McGraw Hill, 569.